Electronic Supplementary Material (ESI) for Journal of Materials Chemistry A.

Supplemental Information

Nanosheet-based Magadiite: A Controllable Two-dimensional Trap for Selective Capture of Heavy Metals

He Ding, Yang Chen, Tianyi Fu, Bai Peng and Xianghai Guo*

Department of Pharmaceutical Engineering, School of Chemical Engineering and Technology, Tianjin University, Tianjin 300350, P. R. China

Key Laboratory of Systems Bioengineering (Ministry of Education), Tianjin University, Tianjin, 300072, P. R. China

*Corresponding author.

^{1}H NMR of C_{22}DMIZ, $CDCl_3$, 500 MHz

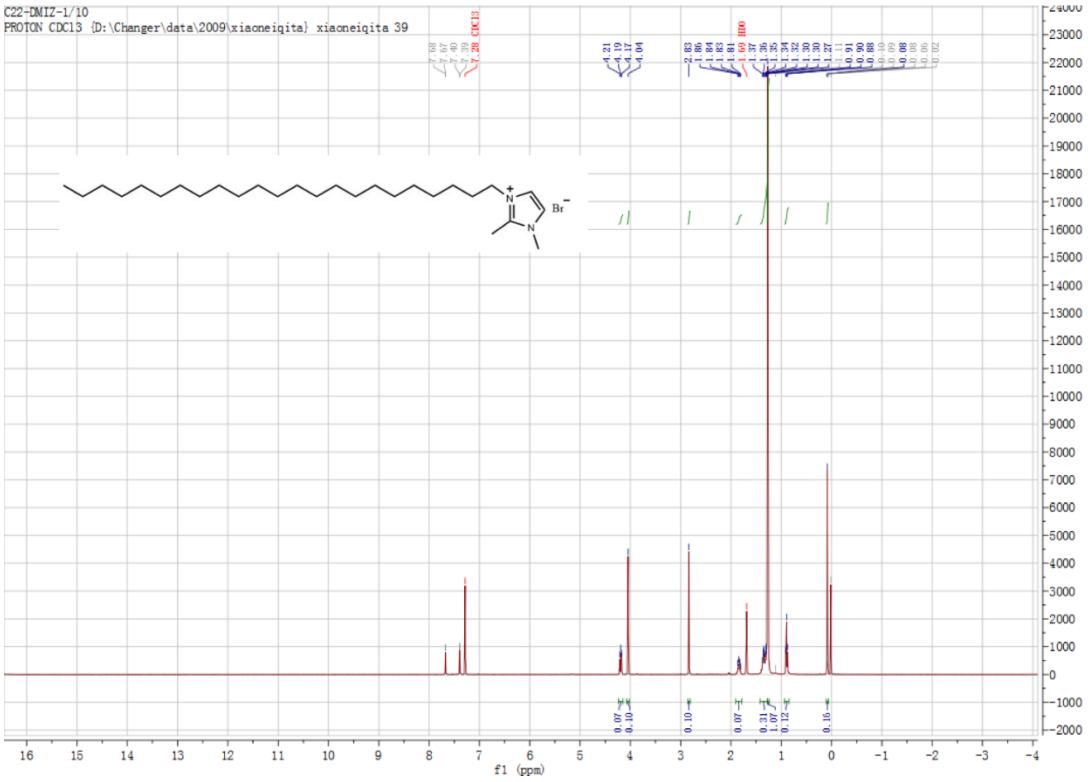

^{13}C NMR of C_{22}DMIZ, $CDCl_3$, 500 MHz

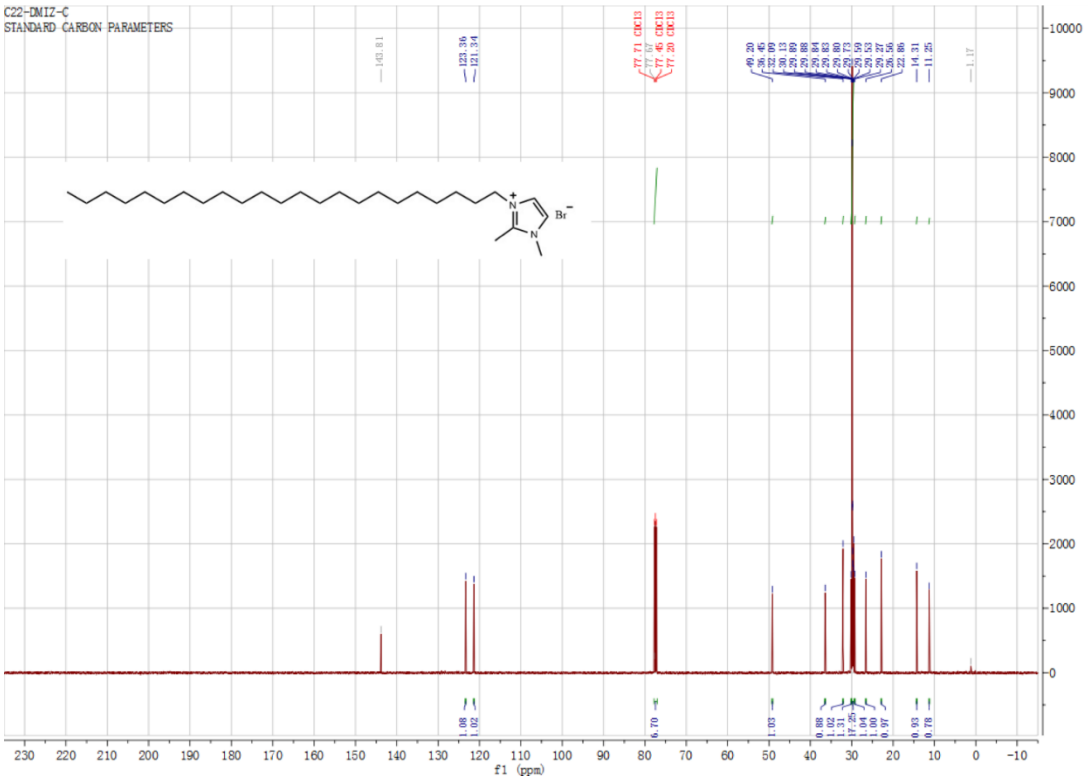

^{1}H NMR of $C_{18}DMIZ$, $CDCl_3$, 500 MHz

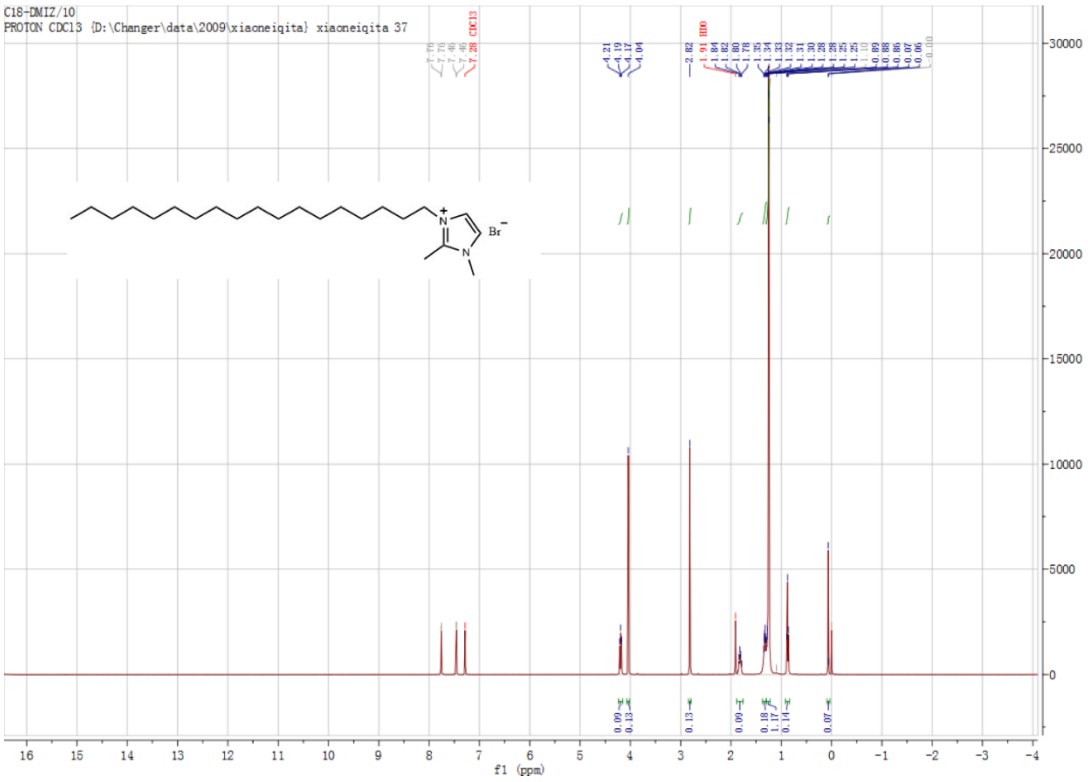

^{13}C NMR of $C_{18}DMIZ$, $CDCl_3$, 500 MHz

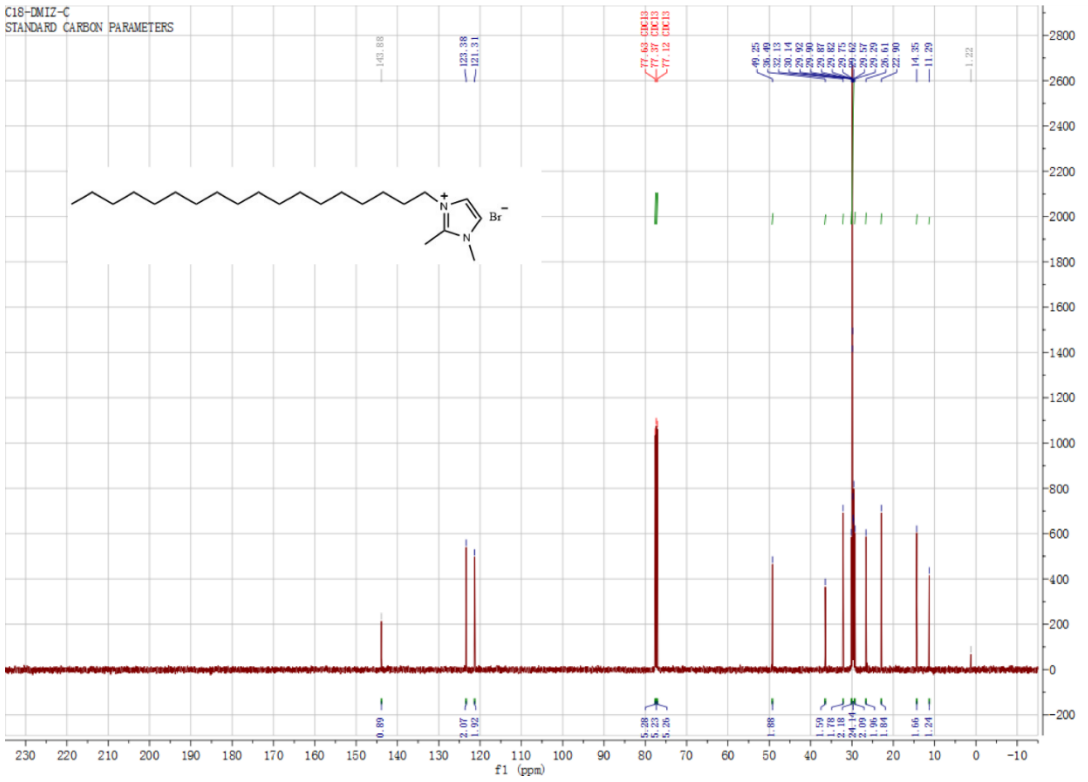

^{1}H NMR of $C_{16}DMIZ$, $CDCl_3$, 500 MHz

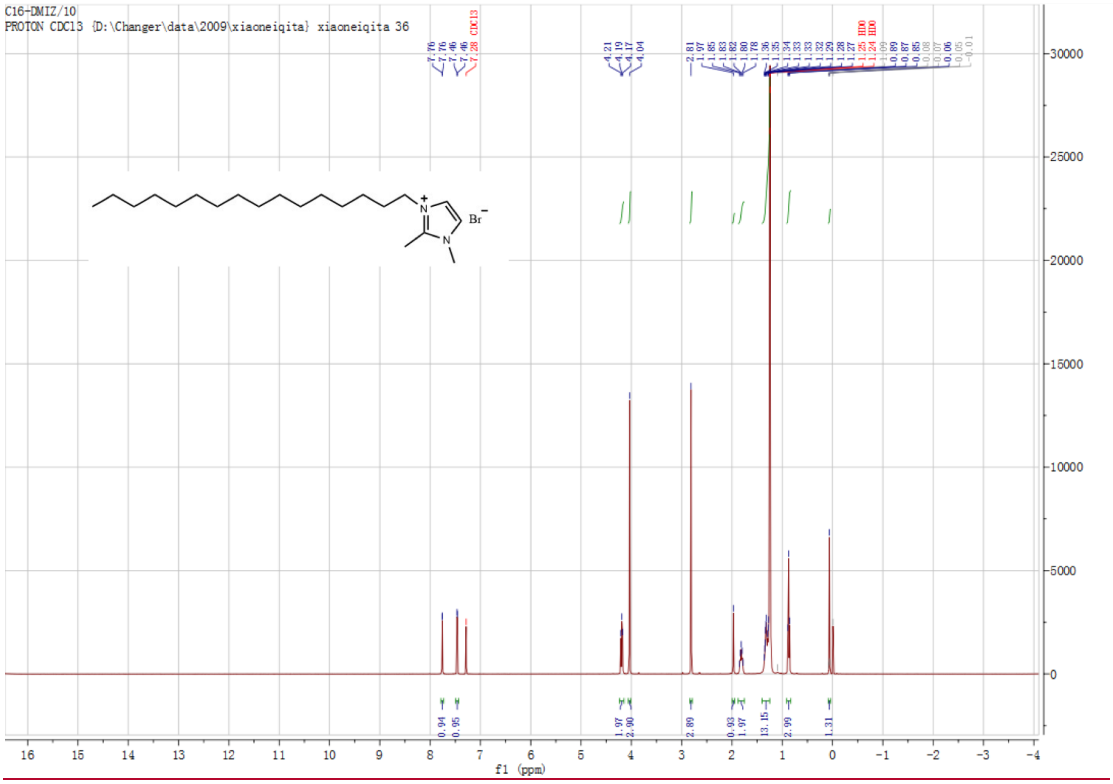

^{13}C NMR of $C_{16}DMIZ$, $CDCl_3$, 500 MHz

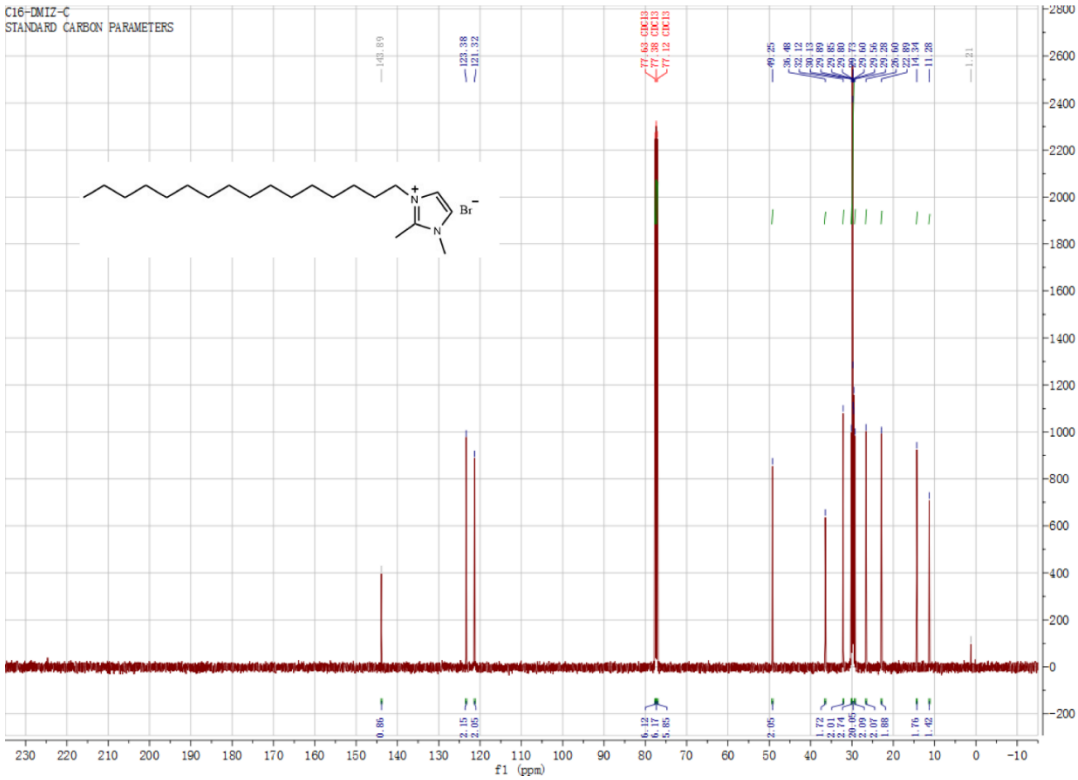

^{1}H NMR of C_{12}DMIZ, $CDCl_3$, 500 MHz

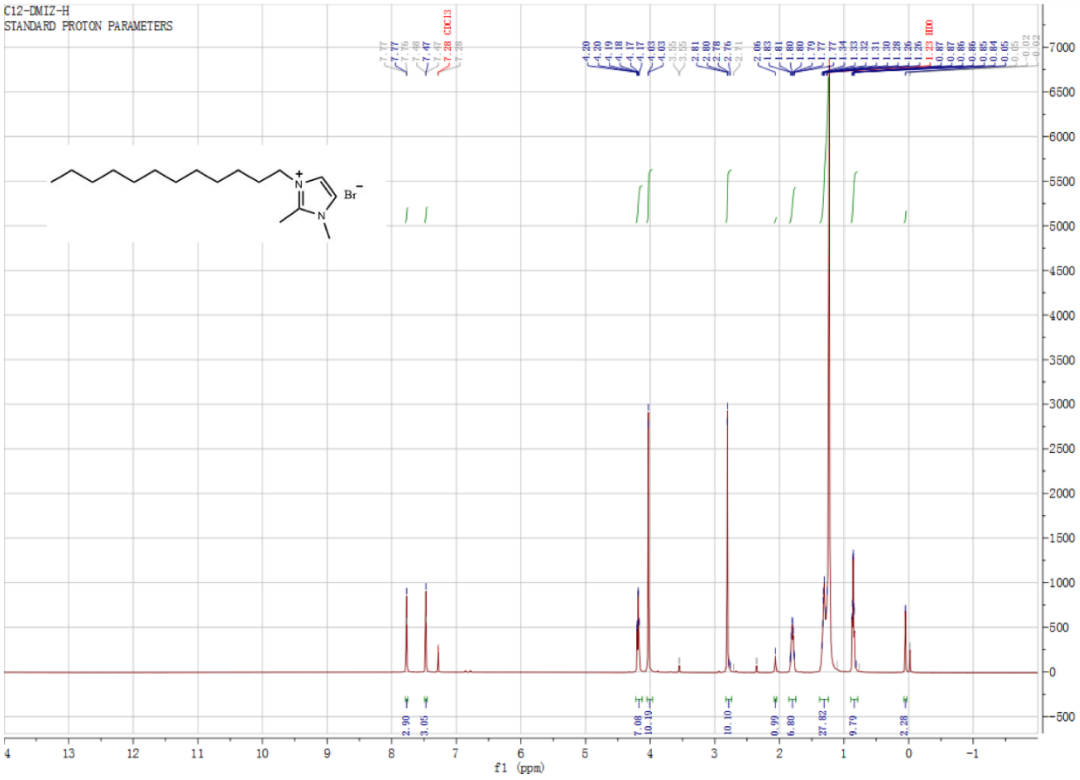

^{13}C NMR of C_{12}DMIZ, $CDCl_3$, 500 MHz

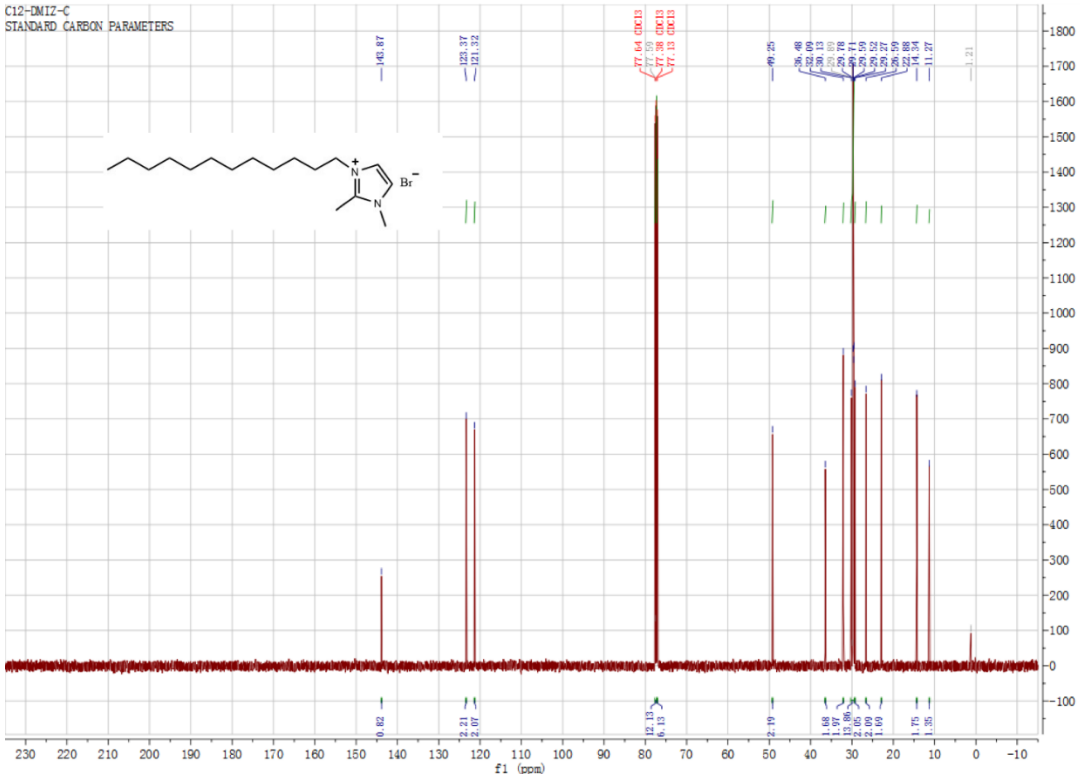

Figure S1. ^{1}H and ^{13}C NMR spectra of OSDAs.

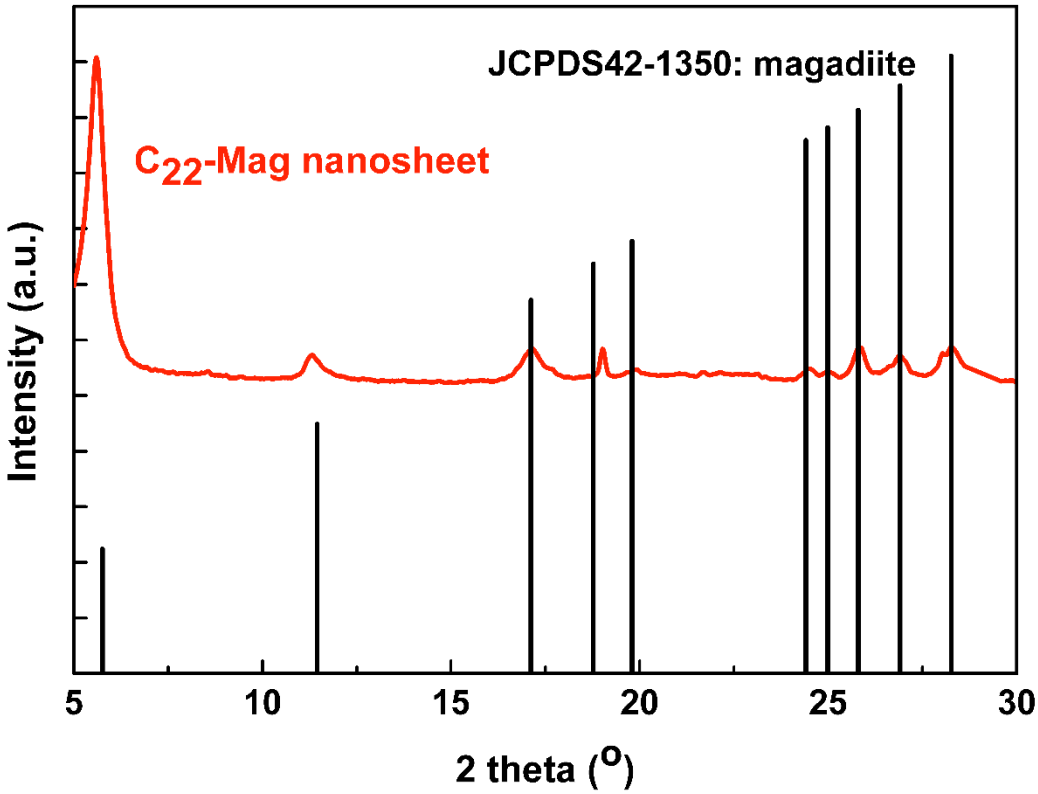

Figure S2. XRD patterns of JCPAS42-1350, magadiite.

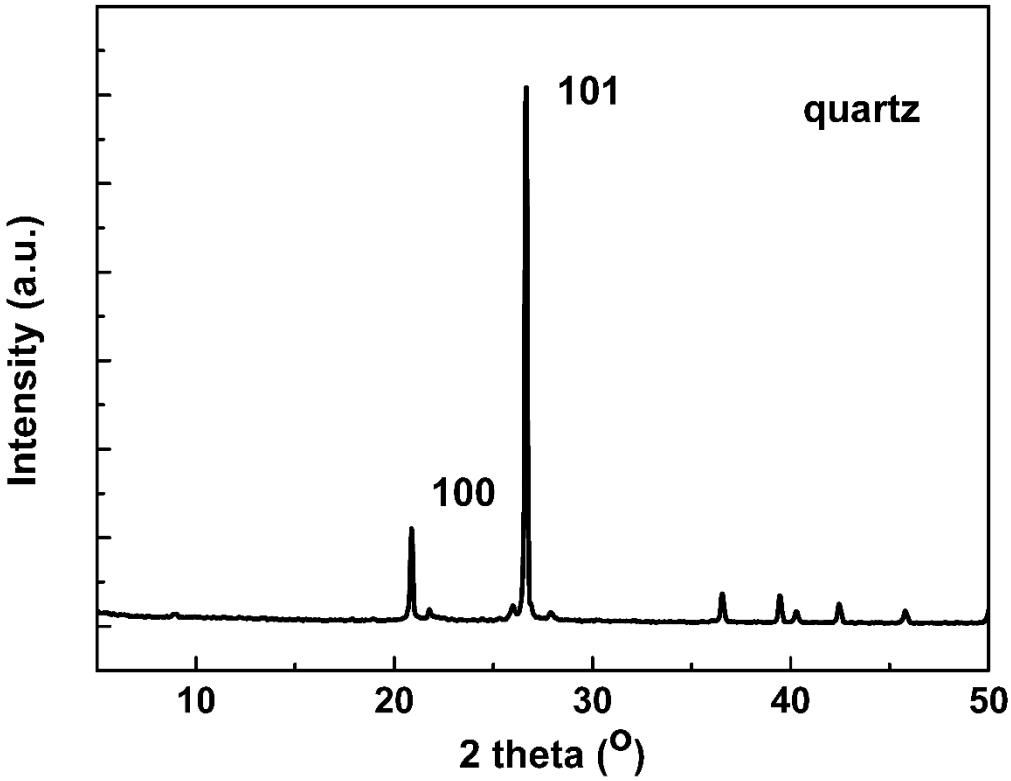

Figure S3. XRD patterns of the CS1 samples.

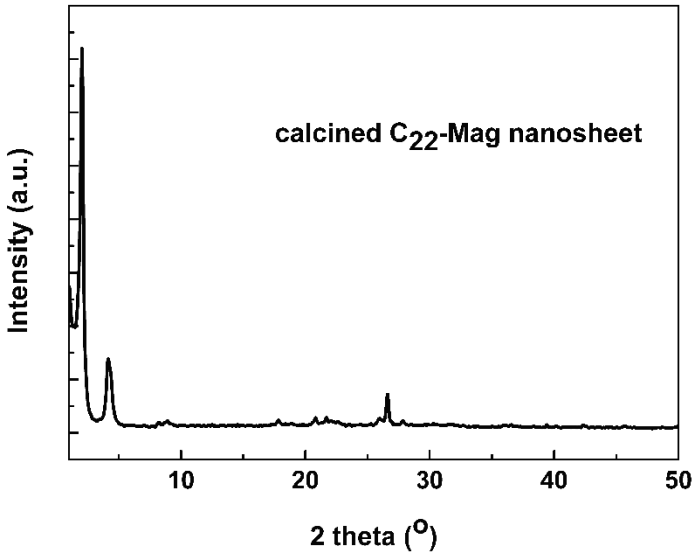

Figure S4. XRD pattern of Calcined C22-Mag nanosheets.

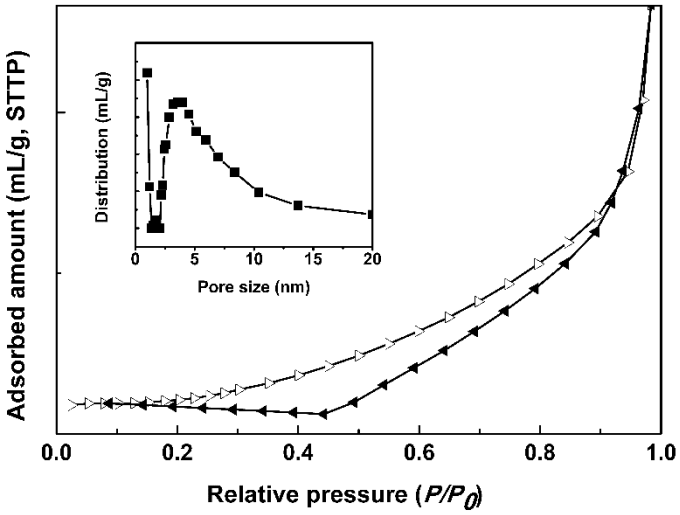

Figure S5. Nitrogen adsorption-desorption isotherm at –196 °C and pore size distribution of the calcined C_{22}-Mag nanosheets.

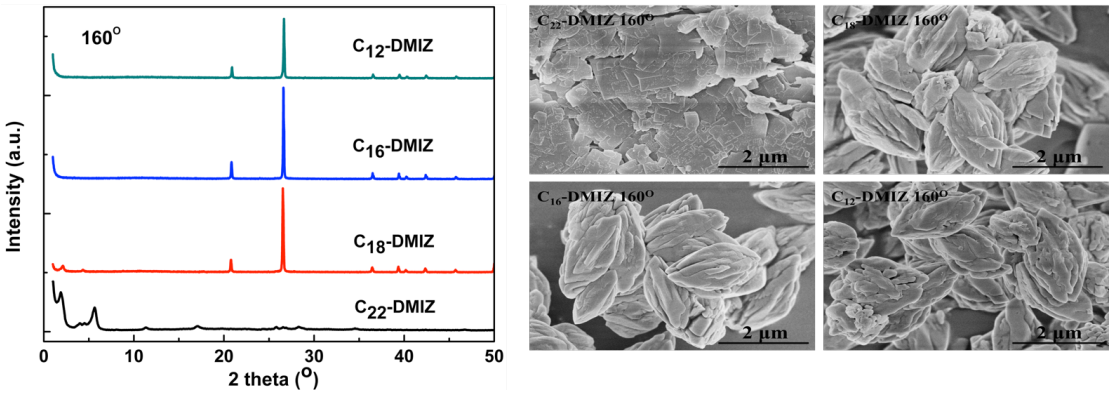

Figure S6. XRD patterns and SEM images of samples directing by imidazolium-based surfactants at 160°.

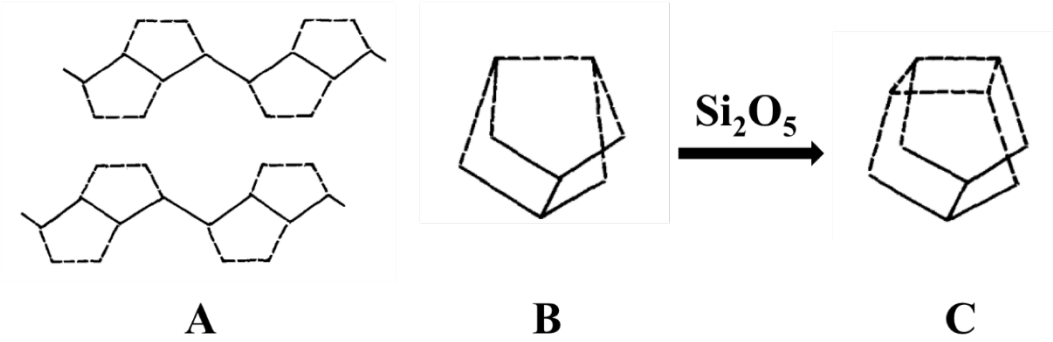

Figure S7. Schematic views of the model structure of magadiite: (A) a-b plane of the dachiardite derived model, (B) type-B block, (C) octosilicate block.

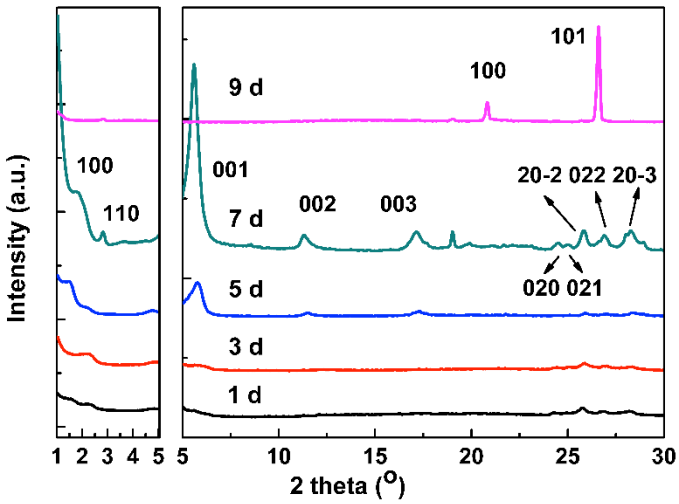

Figure S8. XRD patterns of C_{22}-Mag nanosheets subjected to hydrothermal synthesis for different times: 1 d, 3 d, 5 d, 7 d and 9 d.

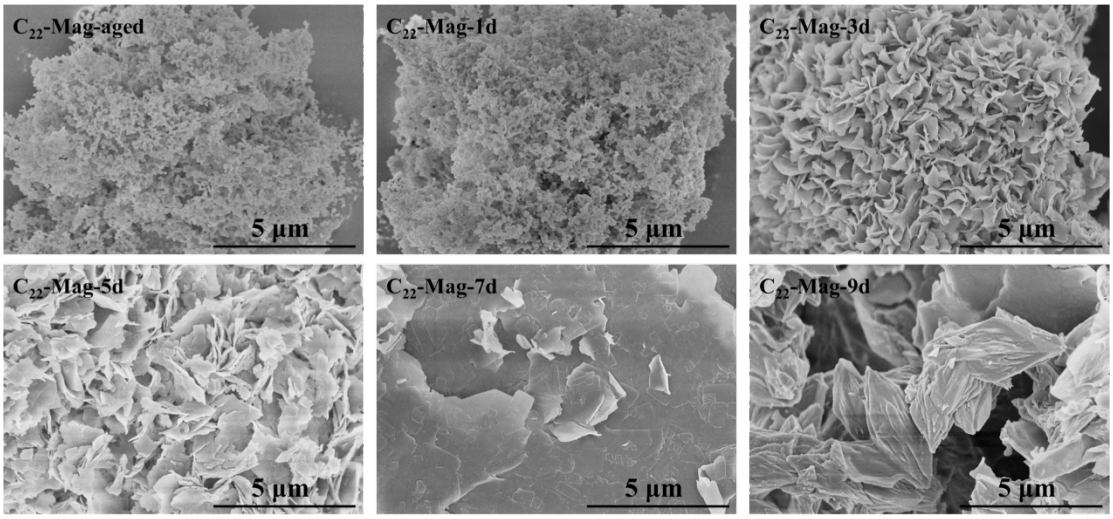

Figure S9. SEM images of C_{22}-Mag nanosheets subjected to hydrothermal synthesis for different times: aged, 1 d, 3 d, 5 d, 7 d and 9 d.

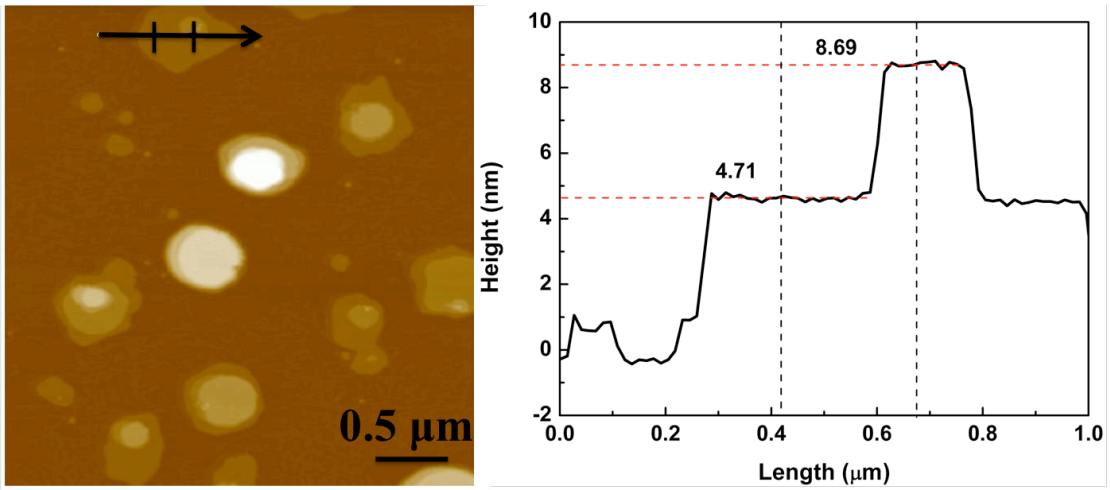

Figure S10. AFM amplitude mode image of calcined C_{22}-Mag nanosheets on Si wafer (left) and height profile along the marked line in AFM (right).

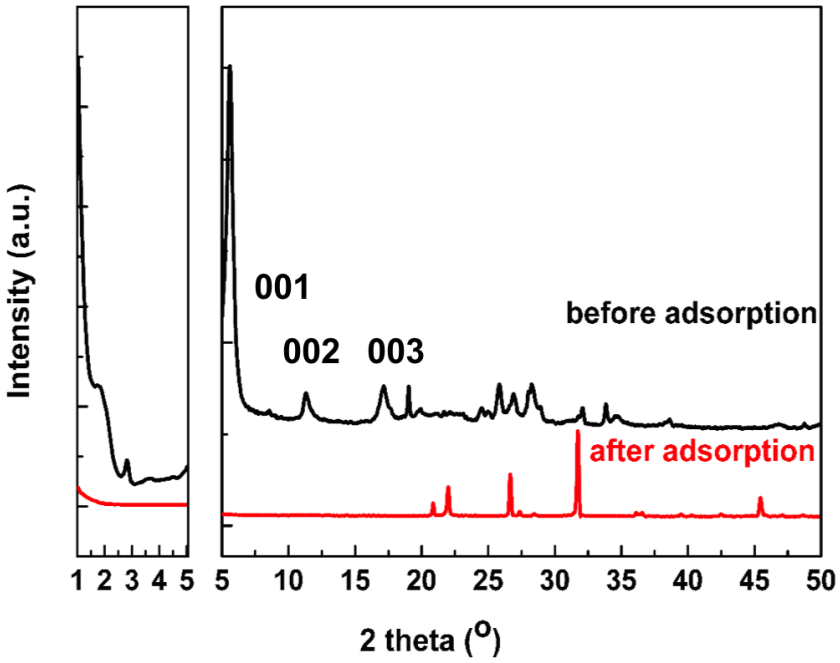

Figure S11. XRD patterns of C_{22}-Mag nanosheet before and after adsorption tests.

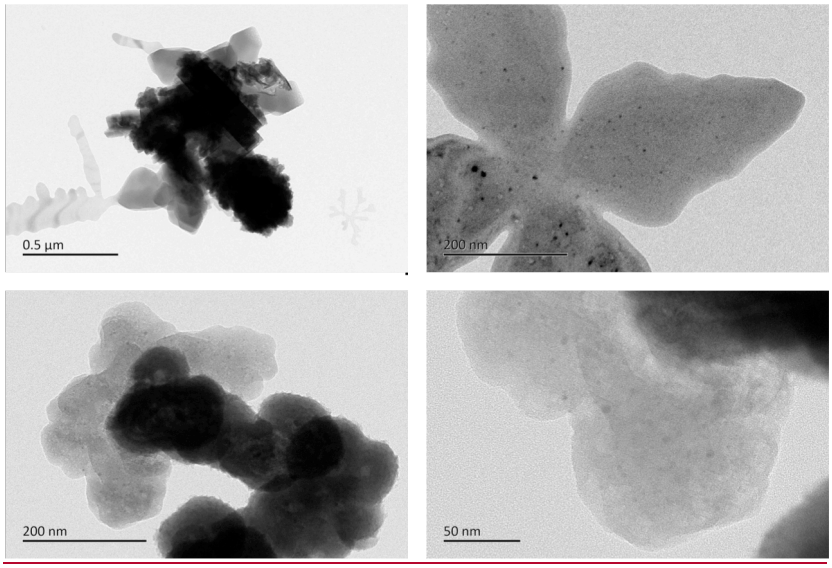

Figure S12. TEM images of C_{22}-Mag nanosheets after adsorption tests.

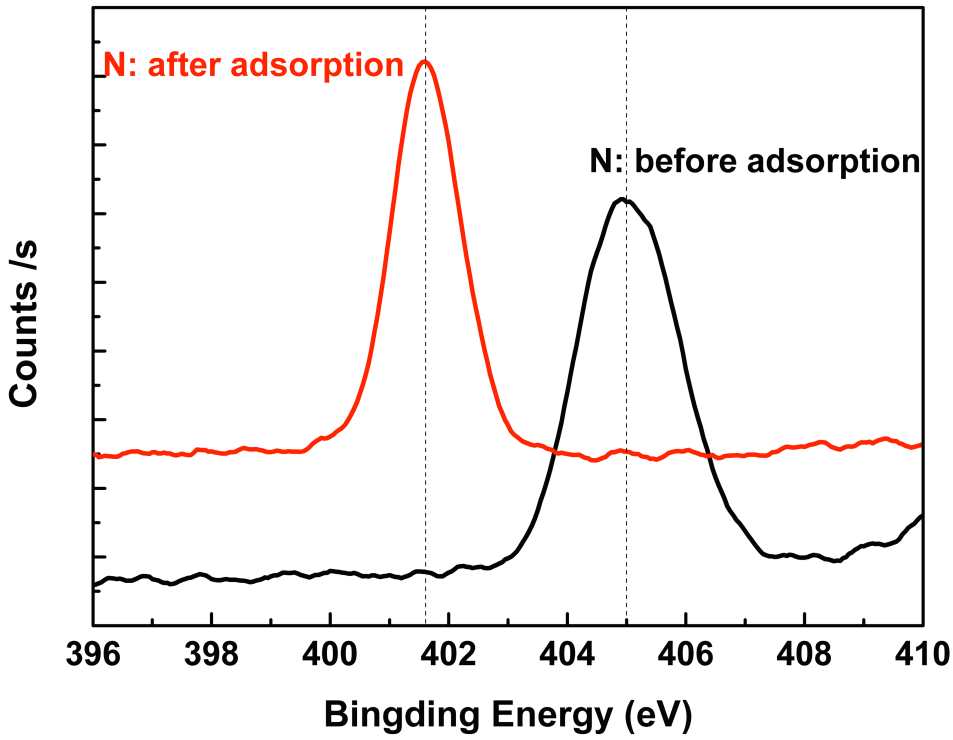

Figure S13. XPS pattern of N element before and after adsorption.

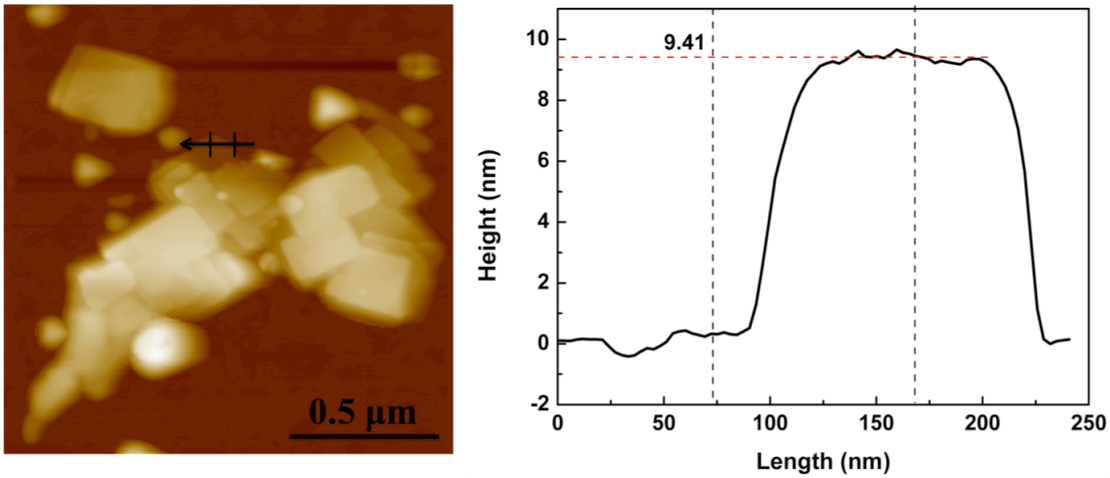

Figure S14. AFM amplitude mode image of C_{22}-Mag nanosheets after adsorption tests on Si wafer (left) and height profile along the marked line in AFM (right).

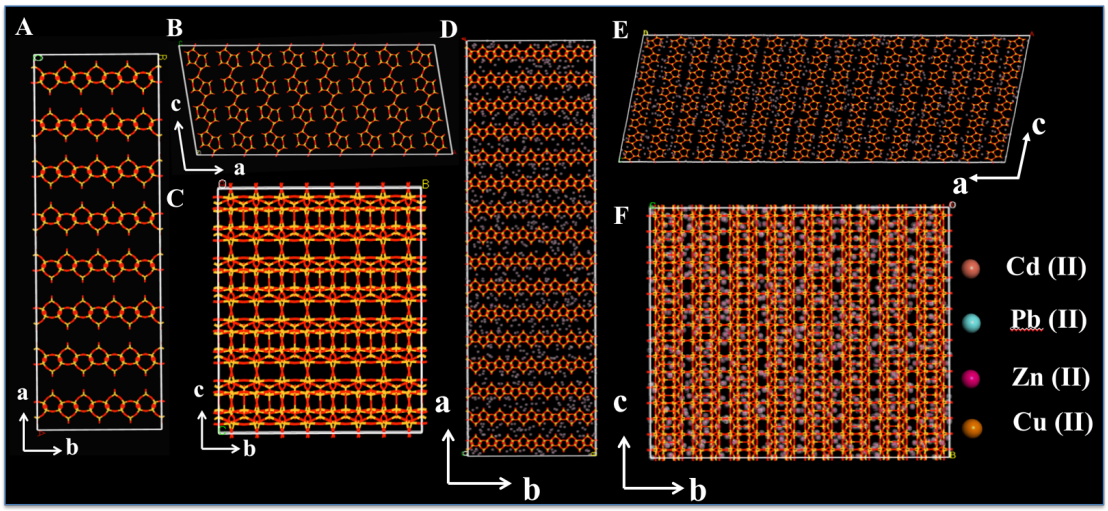

Figure S15. (A, B and C): scheme of raw magadiite nanosheets crystal structure, a: 2.75 nm; b: 0.75 nm; c: 0.92 nm. (D, E and F): scheme of magadiite nanosheets crystal structure after adsorption of heavy metals.

Table S1 Peak temperature of Cx-Mag nanosheets in DTG pattern

Samples	T/°C		
C_{22}-Mag nanosheet	70.00	315.00	351.14
C_{18}-Mag nanosheet	88.40	297.50	354.78
C_{16}-Mag nanosheet	82.10	298.76	353.52
C_{12}-Mag nanosheet	80.84	280.31	375.92

Table S2 Physical characteristics of four kinds of heavy metals.

Metals	RBS[a]	HR[b]	IR[c]	PE[d]	IP[e]	pK_h[f]	HI[g]
Cu (II)	2.66	4.19	0.73	1.90	7.73	7.5	0.104
Pb (II)	2.68	4.01	1.19	2.33	7.42	7.6	0.131
Zn (II)	2.20	4.3	0.74	1.65	9.39	9.0	0.115
Cd (II)	2.15	4.26	0.97	1.69	8.99	10.1	0.081

[a] RBS: relative binding strengths; [b] HR: hydrated radius; [c] IR: ionic radius, [d] PE: Pauling electronegativity; [e] IP: ionization potential; [f] pK_h: negative log of the first hydrolysis constant; [g] HI: hardness index.